LASERLAB-EUROPE

The Integrated Initiative of European Laser Research Infrastructures III

Grant Agreement number: 284464

WP31
Charged Particle Acceleration with Intense Lasers
(CHARPAC)

Deliverable number 31.6

. **Report on stability control of laser-accelerated electrons**

Lead Beneficiary:

Lund Laser Centre, Lund University - LU

Due date: 30.11.2015

Date of delivery: 30.11.2015

Project webpage: www.laserlab-europe.eu

Deliverable Nature	
R = Report, P = Prototype, D = Demonstrator, O = Other	R
Dissemination Level	
PU = Public PP = Restricted to other programme participants (incl. the Commission Services) RE = Restricted to a group specified by the consortium (incl. the Commission Services) CO = Confidential, only for members of the consortium (incl. the Commission Services)	PU

A. Abstract / Executive Summary

The advances in CHARPAC on the stability control of laser-accelerated electrons is presented with a detailed discussion on the experimental progress obtained on the improvement of the LWFA beams in capillaries and the determination of the key beam parameters for that specific configuration. A new variable length gas cell was developed and characterized, showing very low density fluctuations. Using two independent sources of gas, it is demonstrated that by controlled injection can produce stable, reproducible and tunable electron beams. From a numerical point of view, the implementation of a novel algorithm allowing for numerical studies of very long propagation lengths and thus stability of electron beams over realistic laser plasma accelerator conditions of relevance for multi GeV energies is also described. Finally, progress on a theoretical model to describe self-injection in LWFA and thus determine the trapping conditions is also presented, with the aim of providing a theoretical framework capable of describing the injection conditions that can determine the stability of the beams in the bubble regime.

B. Deliverable Report

1 Introduction

Laser driven acceleration of particles has opened important new perspectives for major applications in science, technology and healthcare. By focusing intense laser pulses onto a target, it is possible to produce high quality and energetic particle beams. However, applications in these areas are hampered by the present limitations of laser–accelerated beams. The control of the beam parameters such as energy, energy spread, divergence, emittance, and current are essential requirements for unraveling and determining potential applications. The aim of this JRA is to address in two tasks several of these important questions for the case of ion and electron beams. **In this report we present the progress in CHARPAC on stability control of laser-accelerated electrons, a critical topic to take laser wakefield acceleration to the realm of applications, in particular in terms of possible biomedical and bioimaging applications.**

The efforts to be deployed in the first task of CHARPAC are focused on the improvement of the properties and the stability of these electron beams, and this report addresses specifically the second critical issue by new ideas and measuring the ultimate stability of the electron beams. Leveraging on the recent improvements in laser chains, the ultimate measurement of the electron beam stability (electron beam stability and reproducibility – shot-to-shot fluctuation of electron energy, energy bandwidth, beam charge, profile and beam pointing minimization) is now possible. Having a very reproducible electron beam is crucial for fine physical studies of the beam/plasma interaction. The role of space charge and the initial phase space volume are also important in connection with the electron beam longitudinal and transverse emittance. The influence of the bubble environment (electric and magnetic fields) is also of significance. **Within CHARPAC, we are reporting already significant progresses on the studies of the improvement of the stability of laser plasma accelerators and on the theoretical models that can support a more detailed understanding of the parameters determining the stability of LWFA beams.**

2 Objectives

The main objective is to improve the plasma wakefield accelerator stability and in helping to evaluate its scalability for future projects of interest to the high-energy physics community, for the design of compact free-electron lasers and their numerous applications, resorting to a combination of experiments performed by the CHARPAC teams supported by state-of-the-art simulations and theoretical models.

3 Work performed / results / description

The presented work is the result from a considerable collaborative effort, involving cooperation and collaboration between many partners in Laserlab-Europe and in the framework of the CHARPAC JRA. The experiments and theoretical studies are aimed at achieving increased control and stability of the laser-accelerated electron beams. The approach is to control and stabilize the most important components of a laser-plasma accelerator: the laser pulse, the plasma source and the electron injection process.

3.1 Stability and control of the laser

An important effort on the **improvement of the stability of laser plasma accelerators** was undertaken by the Lund Laser Centre (LLC-LU). Here we report on a study of the stability of beams of laser-plasma accelerated electrons using dielectric capillary tubes as laser waveguides. The experimental study was performed as a Laserlab access experiment at LLC, and was a collaboration between LLC, LPGP (Orsay, France) and CEA-Saclay.

Dielectric capillary waveguides have the advantage that the plasma density inside the tubes can be arbitrarily low, as the laser beam is then guided purely by reflection from the tube walls. The absence of a minimum density requirement for guiding makes the capillary tube relevant for laser wakefield acceleration over long distance since the maximum achievable electron energy scales with the inverse electron density. The capillary tube also provides a shock-free gas medium which is very important for stable laser propagation and particle acceleration.

The experiments were conducted at the Lund Laser Centre, using a Ti:Sapphire multi-terawatt laser system, set to deliver pulses with energy of 750 mJ and duration of 40 fs. The laser beam was focused to an estimated peak intensity of 4×10^{18} W/cm^2 in a 19 μm (FWHM) focal spot. Controlling the laser pointing is essential when performing experiments in dielectric capillaries to prevent damage to the guiding structure. For this reason, an active pointing stabilization system was developed and used to achieve a short-term scatter of the transverse focal spot position of less than 3 μrad, while any long-term drift was essentially eliminated, see Fig. 1.

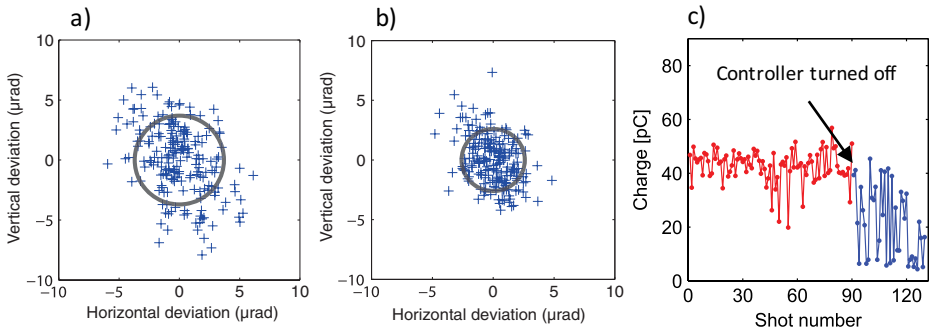

Figure 1: (a) Measurements of the laser pointing in the focal plane, with the stabilization controller turned off, showed fluctuations of 3.7 μrad (RMS). (b) With the pointing stabilization turned on, a laser pointing was improved to 2.6 μrad. (c) With the controller turned on, stable electron beams with average charge of 43 pC were generated using gas-filled capillary tubes. Turning off the controller lead to damage of the capillary tube and significantly larger electron beam fluctuations and eventually a loss of the electron beam.

Electron beams were produced using different glass capillary tubes with diameters in the range 76 to 254 μm and lengths in the range 8 to 20 mm. The leakage from a dielectric mirror in the beam path was used to record spatial and spectral intensity distributions of every laser pulse. A large set of data was acquired for statistical analysis of the electron beam stability and the dependence on experimental parameters. Some results are summarized in Fig. 2. Electron beams with an average charge of 43 pC and a standard deviation of 14% were generated. The fluctuations in charge are partly correlated to fluctuations in laser pulse energy which illustrates the importance of not only stabilizing the pointing but also the laser pulse energy. The pointing scatter of the electron beams is measured to be as low as 0.8 mrad (RMS). High laser beam pointing stability clearly

improved the stability of the electron beams. A comparative study of electron beam stability, summarized in Fig, 3, was performed using several different capillary geometries and a supersonic gas jet. The beams of electrons accelerated in capillary tubes during this experiment were more stable in charge, divergence, and pointing than beams generated in a gas jet. The stable and uniform gas density distribution, which is also shock-free, that can be achieved in a dielectric capillary tube, or a gas cell of similar dimensions, is expected to contribute to this stability of the resulting electron beams.

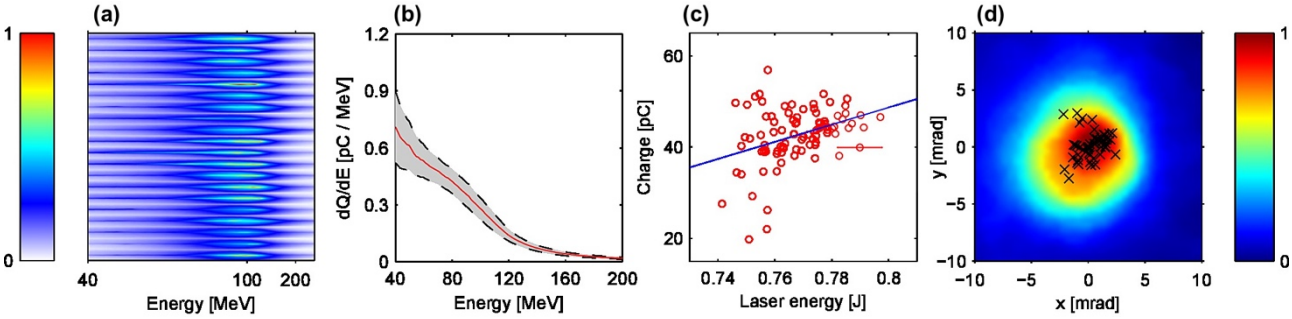

Figure 2: (a) False color images of the dispersed electrons on a scintillating screen from 15 consecutive shots, all using the same colorscale. (b) The average electron spectrum of all 90 shots in the sequence is plotted as a solid red line. The shaded area, bounded by dashed lines, shows the corresponding standard deviation from the average spectrum. Over the full energy range, the maximum standard deviation from the average spectrum is 27%. In (c), the charge of the electrons in the beam, with energy above ~40 MeV, is plotted as a function of laser pulse energy for 90 consecutive shots. The estimated measurement error in laser energy of 1% is marked as a solid red line only in one data point for clarity. This figure shows a clear correlation to laser energy. In (d), a typical beam profile is shown together with a scatter map of the centroids of a sequence of 30 shots.

Parameter	A	B	C	Gas jet
ø [μm]	152	178	254	···
l [mm]	20	10	10	3
$\langle Q \rangle$ [pC]	43	88	107	68
std (Q) [%]	14	14	18	55
$\langle \theta \rangle$ [mrad]	11	10	10	14
std (θ) [%]	13	14	11	64
$\langle \phi \rangle$ [mrad]	1.2	···	0.8	4.4

Figure 3: Summary of electron beam stability parameters acquired in three series using capillaries of different diameter (ø) and lengths (l) (A–C) in comparison with one series of data acquired using gas jet. The stabilities of the electron beams were studied using the same regime of acceleration. Before acquiring each series of data, the experimental conditions were optimized for best stability, yielding slightly different values of, e.g., backing pressure and laser intensity. The average and standard deviation of charge (Q) corresponds to electrons with an energy above 40 MeV measured with the dispersing dipole magnet in the electron beam path. The divergence (θ) and the RMS pointing stability (φ) was measured without the dispersing dipole in the electron beam path.

3.2 Stability and control of the plasma

In experiments on laser wakefield acceleration, laser pulses are typically focused onto gas targets, which are either pre-ionized or become ionized by the laser field. Such experiments depend highly on the density of the target. For stable and reproducible acceleration of electrons, homogeneous density distribution of the target in the interaction region is typically desired. Motivated by the comparative study presented in Section 3.1, **a new variable length gas-cell for stable electron acceleration**, was developed at LLC. The cell consists of two cylinders which can move with respect to each other, see Fig. 4. The main laser beam enters and exits the cell through two 100 µm diameter holes in 500 µm thin sapphire windows. The distance between the inner surfaces of the sapphire windows can be changed in the range 0-15 mm. Glass windows allow optical access transversely to the main beam optical axis. The gas cell was characterized in collaboration between LLC and LOA-ENSTA. In the experiments it is important to know exactly the density at the time the laser pulse is fired into the cell. It is

therefore necessary to measure the gas filling time and the gas density, for different gas species (primarily helium and hydrogen), for different lengths and reservoir backing pressures. This was done in a precise and reliable way using optical interferometry. The cell was placed in a vacuum chamber, in one arm of a Mach-Zender interferometer, see Figure 4b. When gas is injected, the optical path difference change and thus also the intensity on the photodiode after the interferometer. By analyzing and unwrapping the time-dependent signal from the photodiode, it is possible to deduce the time-dependent gas density filling curve. The measurements showed that the density in the gas cell reached a stationary state after ~50 ms, although the filling time was weakly density dependent. The filling time was also the same for both hydrogen and helium gas. At the stationary state, 90% of the reservoir pressure was obtained in the cell. The density in the cell was reproducible and 50 consecutive measurements gave the same result within only 0.6% RMS fluctuation, see Figure 4c. These results are very promising and the gas cell, developed and characterized in the frame of the CHARPAC JRA, is now ready to be used for laser-plasma acceleration experiments.

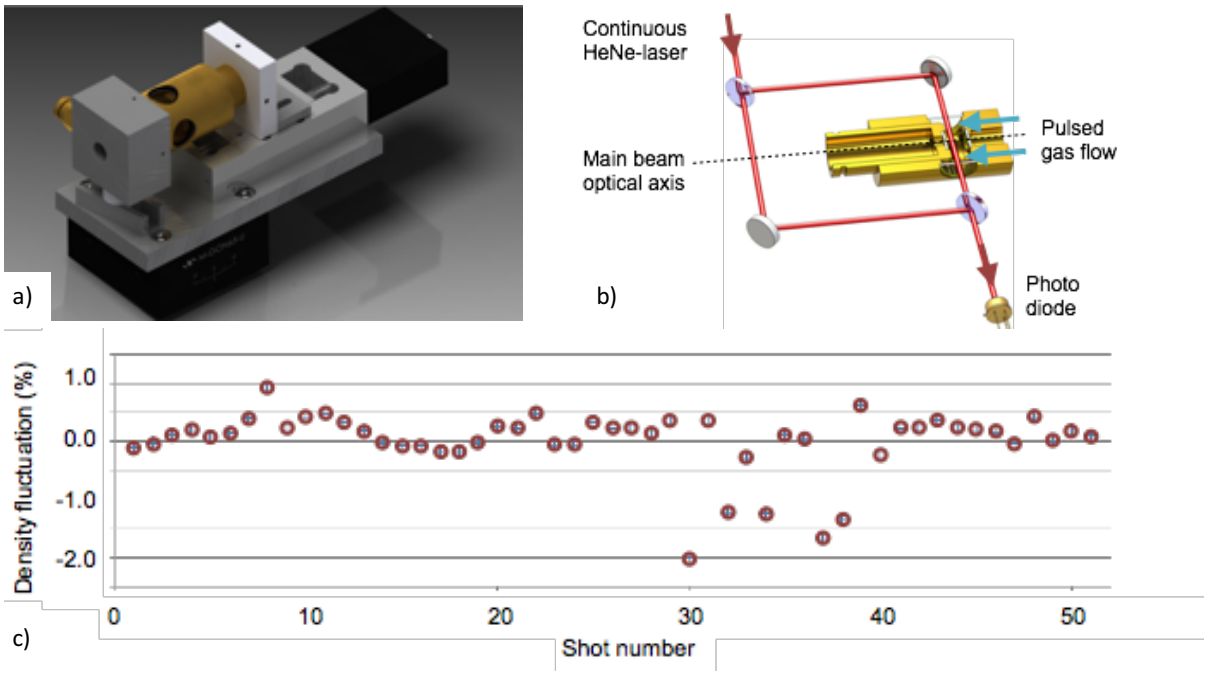

Figure 4: (a) 3D rendering of the variable-length gas cell. (b) Experimental setup to characterize the gas density and filling time. (c) Reproducibility of the gas density was measured to be ±0.6% (RMS).

3.3 Stability and control of the electron injection

In a laser-plasma accelerator, the interaction between the laser and the plasma is strongly non-linear. Small fluctuations in the laser pulse parameters or the plasma density can lead to significant fluctuations in the electron beam emerging from the interaction. One route towards minimizing fluctuations is to lower the density and control the injection and trapping of electrons in the plasma wave. Controlled injection is a very important subject and several different schemes for controlled injection were explored in detail during the CHARPAC JRA, and it is also the main subject of the deliverable report 31.5. Here we focus on the **improvement in electron beam stability using controlled injection**. The activities at the Lund Laser Centre (LU-LLC), focused on the density down-ramp injection mechanism. The physics of this technique is explained in detail in deliverable 31.5 “Report on the injection schemes studies”. Here we explain the experimental setup for density down-ramp injection that was used at the LLC, and the degree of electron beam stability that was obtained. The laser pulses, each containing 650 mJ of energy and with a duration (FWHM) of 40 fs, were focused to an almost circular spot with 19 μm diameter (FWHM), using an *f*=765 mm off-axis parabolic mirror. The peak intensity of the laser pulses, when focused in vacuum, was determined to 3.7×10^{18}

W/cm^2, corresponding to a normalized vector potential of 1.3. The laser pulses were focused on the front edge of a gas jet provided from a 2 mm nozzle with its orifice located 1 mm from the optical axis. A narrow, 0.4 mm diameter tube was inserted into the jet, with its orifice 0.2 mm from the optical axis, providing locally an additional amount of gas. The measured total density distribution, shown in Fig. 5b, contains a peak and a plateau joined together by a 230 μm long down-ramp. Under suitable chosen conditions, density down-ramp injection of electrons into the accelerating phase of a laser plasma wakefield occurs in this gradient and the electrons are subsequently accelerated in the remaining plasma.

Electrons were first injected and accelerated in a target where gas was supplied only from the 2 mm gas nozzle. The threshold in electron number density in the plateau for required self-injection was found to be approximately 11×10^{18} cm^{-3}. The observed beams of electrons had the typical characteristics of self-injection in gas jets, with limited reproducibility and a bunch charge of the order of 30 pC with a standard deviation higher than 50%.

The electron number density provided from the 2 mm nozzle was lowered well below threshold for injection (to 3×10^{18} cm^{-3}). When adding gas also from the narrow tube, beams of accelerated electrons were observed for 100% of the laser pulses sent onto the target. The bunches of accelerated electrons injected using this composite gas target contain only of the order of 1 pC and their spectra typically contain a broad peak (see Fig. 5c). Furthermore, the shot-to-shot stability in charge and energy of the electron beams, with standard deviations 13% and 5%, respectively, is far better than the stability of the beams injected through the self-injection mechanism in a single gas jet. The very high degree of shot-to-shot reproducibility is illustrated in Fig. 5d which shows 100 consecutive electron beams.

In addition to improving the stability, this scheme also allows precise control of the electron beam charge and peak energy. The amount of charge in the electron beams could be controlled, within a certain range, by varying the peak density while keeping the plateau density constant (see Fig. 5e). The kinetic energy of the accelerated electrons could be separately controlled by moving the 2 mm gas nozzle, while keeping the position of the down-ramp fixed with respect to the laser focus in vacuum. The resulting dependence of the peak electron energy on the length of the remaining plasma is shown in Fig. 5f for two different densities in the plateau. The average accelerating electric field is estimated by fitting a line to each series of data. This gives a value of 37 MV/mm at a density of 2.6×10^{18} cm^{-3} in the plateau and 50 MV/mm at a density of 3.25×10^{18} cm^{-3}.

Numerical simulations were performed to support the experimental findings and to further explore the physics of density down-ramp injection. The simulations were performed at CEA-DAM using the Calder-CIRC particle-in-cell code. As a direct and very positive result from the CHARPAC JRA meetings, an agreement was made between LLC, LOA, and CEA, to use the Calder-CIRC code for plasma simulations on computing resources in Sweden. The simulation results, summarized in Fig 6, show that the laser pulse undergoes self-focusing and self-compression and drives a highly nonlinear plasma wave when the pulse reaches the density peak. However, no electrons are injected into the accelerating structure in this region (see Fig. 6b). In the density down-ramp, the wakefield structure increases in size and a certain portion of the background electrons become located within the electron void behind the laser pulse (see Fig. 6c). The injection of electrons into the wakefield stops when the rear end of the first plasma period reaches the end of the density down- ramp, whereas the already injected electrons become further accelerated in the remaining plasma.

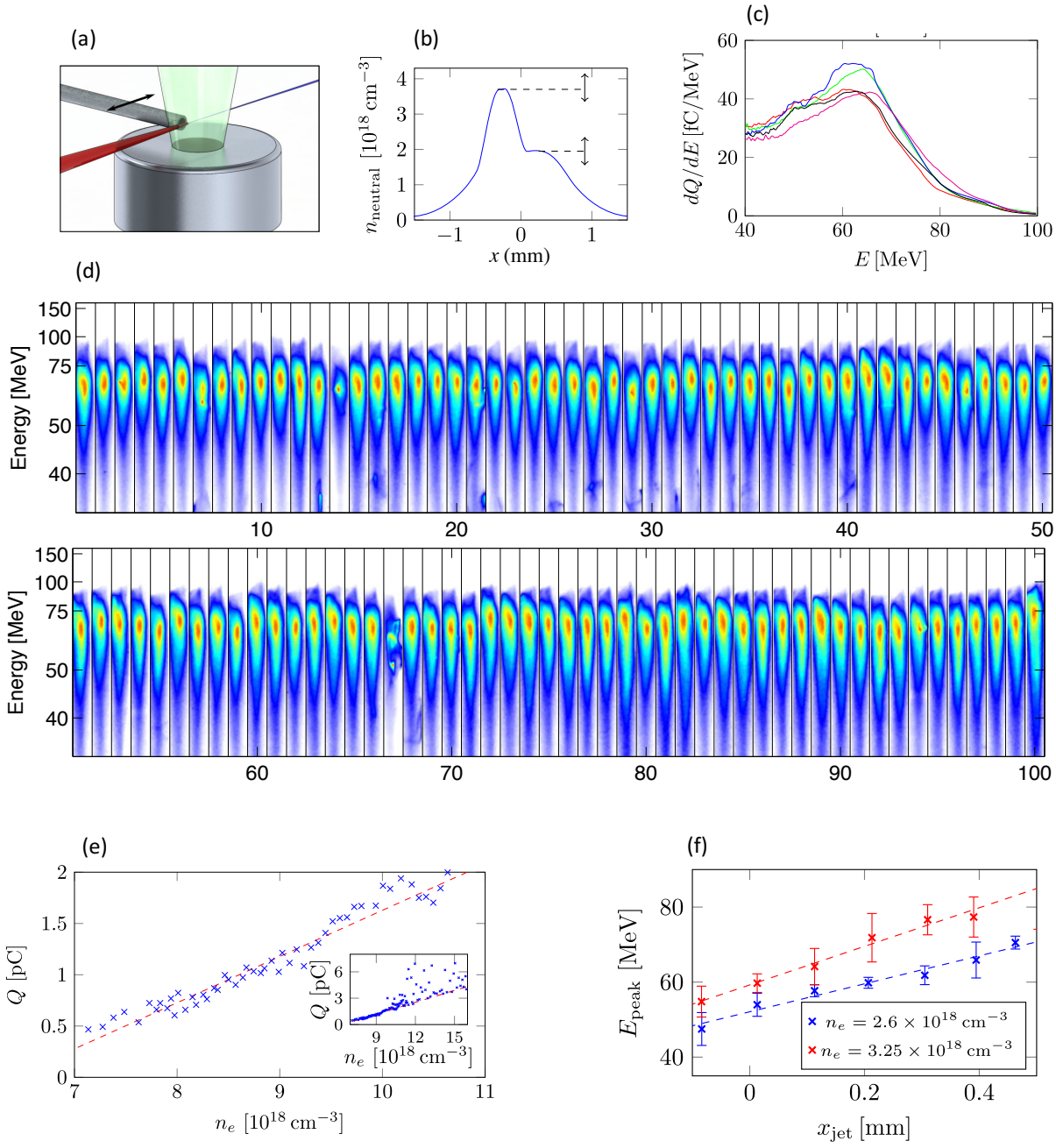

Figure 5: (a) Schematic illustration of the experimental setup for controlled injection using two sources of gas. (b) The typical neutral gas density distribution, along the optical axis, consists of a peak and a plateau, separated by a density down-ramp. The tube can be moved along the optical axis to change the position of the density peak and thus also the density down-ramp. Furthermore, the density in the peak and plateau can be varied independently. (c) Energy spectra from 5 consecutive measurements. (d) 100 consecutive images of the dispersed electrons impacting on the scintillating screen behind a bending magnet, illustrating the high degree of shot-to-shot stability that was obtained using this method for injection. (e) The charge, above 40 MeV, is controlled by changing the density in the peak

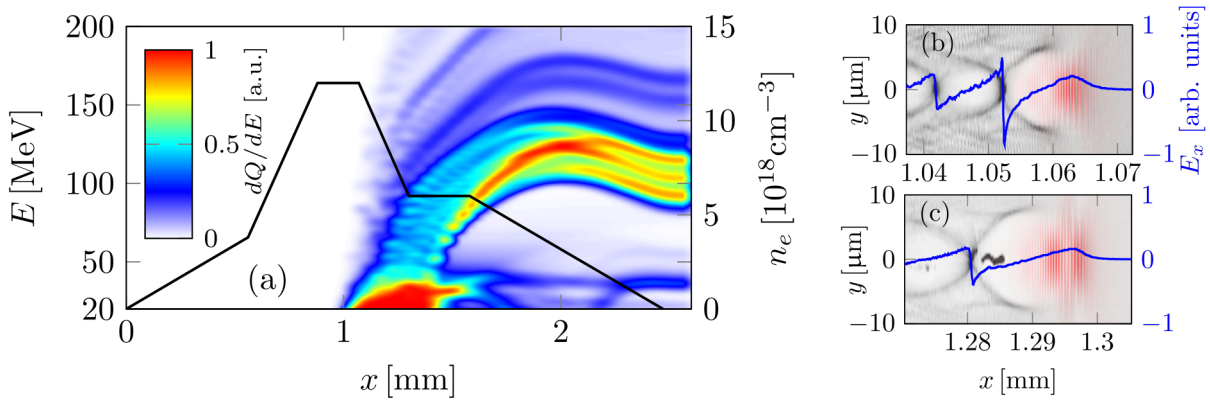

Figure 6: (a) Simulated evolution of the electron spectrum as the laser pulse propagates through the plasma and local electron number density distribution before (b) and after (c) the density down-ramp along with the laser field (red) and accelerating electric field (blue). Injection of electrons into the wakefield structure occurs in the density down-ramp, located between ≈1.1 mm and ≈1.35 mm. The injected electrons are accelerated in the density plateau and the final electron energy spectrum contains a peak centered around 105 MeV and a FWHM of 20 MeV. In (c) electrons have been trapped after being injected as the plasma wavelength gradually increased in the density down-ramp.

3.4 Numerical simulations and theoretical analysis

Full particle-in-cell (PIC) simulations of laser wakefield acceleration need to accurately resolve very short distances on the order of the laser wavelength (~1 micrometer) for comparatively long propagation distances ranging from a few millimetres (for proof-of-principle experiments) to a few meters (for experiments aiming at reaching the energy frontier). This modeling is critical to understand all the parameters that affect the stability of the LWFA. These disparate scale lengths lead to numerically demanding simulations which can be challenging even the largest available supercomputers. **Development of new techniques capable of reducing the computational requisites for** these **simulations** is thus important **to design and to understand current and future experiments focused on the stability of LWFA**. Several techniques have been developed for this purpose, including the use of the Quasi-Static Approximation, which is valid when the laser pulse profile changes can be neglected during the transit of plasma electrons across the laser pulse. Although this approximation is very effective to explore external injection regimes, it nevertheless precludes the physics of self-injection. An approach allowing for large computation speed-ups without physical approximations (i.e. also including self-injection) is the boosted frame technique. Although promising results have been achieved, these simulations are very challenging because of numerical instabilities associated with ultra-relativistic plasma streams in a grid. In order to relax computational requirements, while retaining the physics of self-injection, at the expense of assuming an envelope approximation for the laser pulse, we implemented a ponderomotive guiding center (PGC) laser solver and particle pusher in Osiris.

The PGC approximation is valid as long as the laser pulse frequency remains within 50 % of its initial central frequency, a valid assumption for most of the acceleration in LWFAs. Since only the laser pulse envelope (but not its wavelength) needs to be resolved under the PGC approximation the cell size on the laser propagation direction can be much larger in comparison to full PIC simulations. Computation speed-ups are then associated with the use of lower resolutions in the laser propagation direction and from correspondingly larger numerical time-steps. Computation speed-ups are similar to those achieved with the boosted frame technique, and scale with the square of the ratio between laser and plasma frequencies. We performed ponderomotive guiding center simulations in Osiris which are in very good agreement with full simulations with no approximations, even in the non-linear blowout regime. This is shown in Fig. 7 which shows a comparison between full PIC Osiris simulations and simulations using the ponderomotive guiding center approximation. In this example, the ponderomotive guiding center simulation uses 10 x less cells in the laser propagation direction

and was almost 100 times faster than an equivalent full PIC simulation. Agreement between both simulation is, nevertheless, very good.

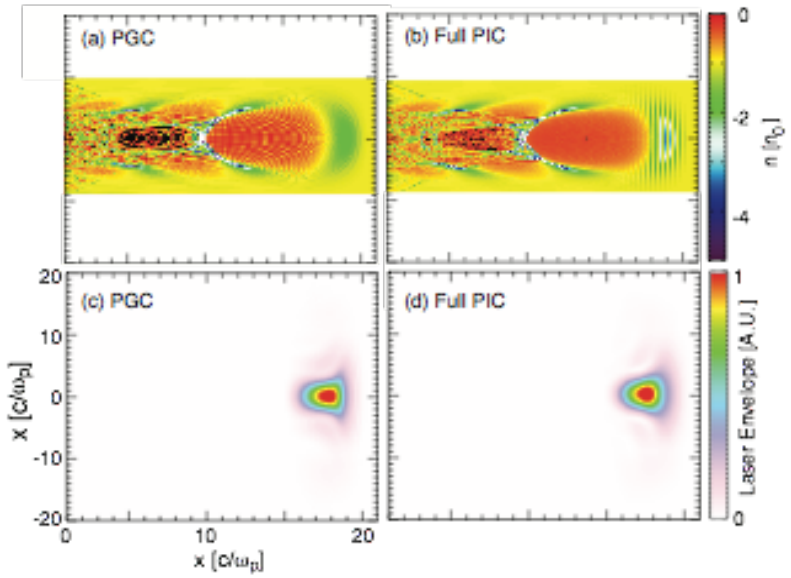

Figure 7: Comparison between PGC approximation and full PIC Osiris simulations of a Laser Wakefield Accelerator. (a) and (b) show plasma electron density for PGC and full PIC. (c) and (d) show corresponding laser pulse intensity profiles.

The dynamics of the bubble also determines the stability of the LWFA beams. Under CHARPAC, the HHUD team studied the **temporal and spatial expansion of a multidimensional model for electron acceleration in the bubble regime**. An extended analytical model for particle dynamics in fields of a highly-nonlinear plasma wake field (the bubble or blow out regime) is derived. The known piecewise model is generalized to include a time dependent bubble radius and full field solution in the acceleration direction. Incorporation of the cavity dynamics in the model is required to simulate the particle trapping properly. On the other hand, it is shown that the previously reported piecewise model does not reproduce the formation of a mono energetic peak in the particle spectrum. The mono energetic electron beams are recovered only when the full longitudinal field gradient is included in the model.

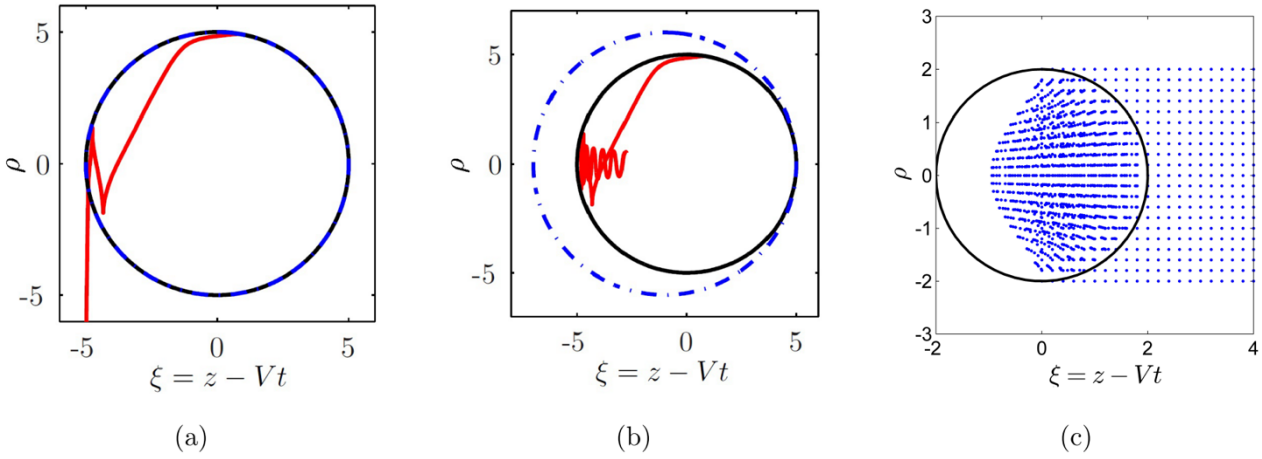

Figure 8: (a) Trajectory in the piecewise model, particle is not trapped. (b) Trajectory in the time-dependent piecewise model, particle is trapped. The black solid circle shows the initial bubble radius R_0. The blue dotted circle is the bubble after the simulation ends. (c) Simulation configuration: Bubble running into a grid of electrons.

To analyse the energy spectra in the time-dependent piecewise model a grid of electrons with zero momentum is placed in front of the bubble (see Fig. 8c). Afterward, we solve the equations of motion for every individual particle, i.e. we neglect the interaction of the test electrons. The electron spectra we receive after the electron bunch of trapped electrons has passed its acceleration length look like that in Fig. 8a. Here, we do not observe any mono energetic

electron beams but a quasi-equal distribution of the particles in energy. The mono-energetic spectra can be recovered in the full gradient model. The full gradient model is however quite difficult to treat analytically. Thus, we introduce another extension of the time-dependent piecewise model that is still analytically treatable and preserves a production of mono energetic electron beams. In the half-pieceweise model (hPWM) we still replace the perpendicular field $E_\perp$ by the constant field-strength parameter F. In longitudinal direction, however, we take the full field gradient. The resulting wake-field potential is

$$\Phi(\mathbf{r}) = \frac{\xi^2 + 2F\,|\,\rho\,|}{4} - \frac{R^2}{4}$$

Here, the coordinate $\xi = z - V\,t$ always contains the group velocity of the generating laser pulse at the bubble front because the bubble radius is assumed to be fixed. If we now repeat the simulations of the electron grid in the the hPWM, we get energy spectra similar to those shown in Fig. 9. As we see, both PIC-simulated spectra in Fig. 9b and our spectrum from a simulation with $F = 4$, $R_0 = 8$, and $\gamma_0 = 15$ exhibit the same structure.

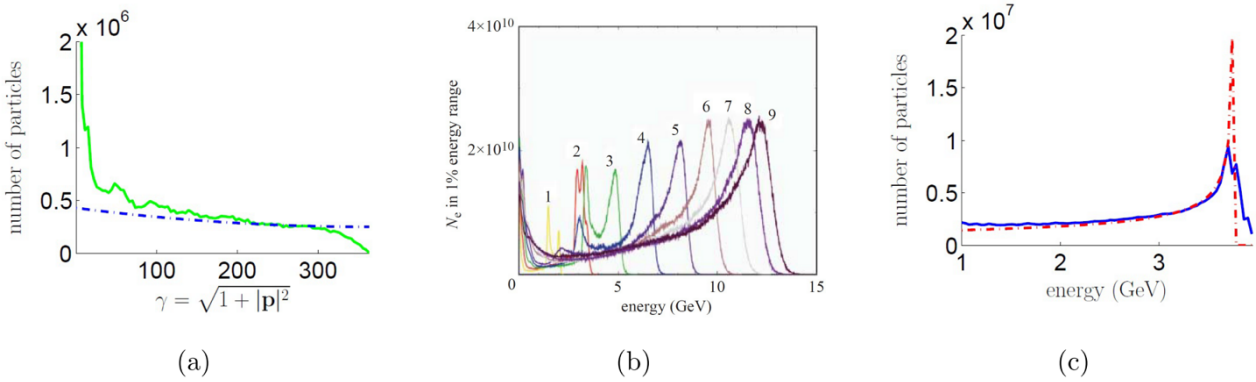

Figure 9: (a) Energy distribution for $F = 4$, $R_0 = 4$, and $\gamma_0 = 5$ in the time-dependent piecewise model. (b) PIC energy spectra taken from Fig.2 in [A. Pukhov and S. Gordienko, Phil. Trans. R. Soc. A 364, 623 (2006).]. (c) Energy spectra in the hPWM for $\gamma_0 = 15$, $R_0 = 8$, and $F = 4$.

Summarizing our expansions of the original piecewise model we note two things. First, we see that it is possible to treat an enhanced interaction between the electron bunch and the bubble potentials. This in turn leads to a growing trapping cross-section and thus to a more efficient self-injection.

Energy spectra in our simulations show that no mono energetic electron beams are generated, if all field gradients are neglected. To fix this problem, we invent a hybrid model that includes the right fields in moving direction and replaces the transverse field gradients by a field strength parameter. In this modification we observe the generation of mono energetic electron beams and are able to calculate trapping conditions analytically.

The next steps of our work will be to go back to the original full gradient model and to try to find the envelope approximation functions by other means than the introduction of a field strength parameter. If we succeed, trapping cross-sections and trapping conditions for the most physical model will be available without thinking about an arbitrarily set field strength parameter.

4 Conclusions

In CHARPAC, an important focus of the activity was on the improvement of the stability of laser plasma accelerators. An experimental effort on LWFA in capillaries was able to demonstrate electron beams with an average charge of 43 pC and a standard deviation of 14%, with the fluctuations in charge are partly correlated to fluctuations in laser pulse energy. The pointing scatter of the electron beams was measured to be as low as 0.8 mrad (rms), also with a correlation between the high laser beam pointing stability and the stability of the electron

beams. A new variable length gas cell was developed, which allows reproducible gas density profile within only 0.6% fluctuations. Controlled density down-ramp injection was used to obtained stable electron beams with fluctuations of 13% in charge and 5% in peak energy. The scheme was also used to demonstrate tunable electron beams (control of charge and peak energy). A new numerical technique to explore the stability of LWFA beams in realistic configurations e.g. long propagation distances was also implemented in one of the PIC codes in use in CHARPAC. A temporal and spatial expansion of a multidimensional model for electron acceleration in the bubble regime was also pursued, including an extended analytical model for particle dynamics in fields of a highly-nonlinear plasma wake field (the bubble or blow out regime) which can predict particle trapping and thus the conditions at injection that can perturb the stability of the self-injected beam.

5 Publications

[1] M. Hansson, L. Senje, A. Persson, O. Lundh, C.-G. Wahlström, F.G. Desforges, J. Ju, T.L. Audet, B. Cros, S. Dobosz-Dufrénoy, P. Monot, *"Enhanced stability of laser wakefield acceleration using dielectric capillary tubes",* Phys. Rev. ST Acc. Beams 17, 031303 (2014). DOI: 10.1103/PhysRevSTAB.17.031303

[2] F.G. Desforges, M. Hansson, J. Ju, L. Senje, T.L. Audet, S. Dobosz-Dufrénoy, A. Persson, O. Lundh, C.-G. Wahlström, B. Cros, *"Reproducibility of electron beams from laser wakefield acceleration in capillary tubes",* Nucl. Instr. Meth. Phys. Res. A **740**, 54-59 (2014). DOI: 10.1016/j.nima.2013.10.062

[3] G. Genoud, M. S. Bloom, J. Vieira, M. Burza, Z. Najmudin, A. Persson, L. O. Silva, K. Svensson, C.-G. Wahlström, and S. P. D. Mangles, *"Increasing energy coupling into plasma waves by tailoring the laser radial focal spot distribution in a laser wakefield accelerator",* Phys. Plasmas **20**, 064501 (2013). DOI: 10.1063/1.4810795

[4] C. Ciocarlan, S. M. Wiggins, M. R. Islam, B. Ersfeld, S. Abuazoum, R. Wilson, C. Aniculaesei, G. H. Welsh, G. Vieux, and D. A. Jaroszynski, *"The role of the gas/plasma plume and self-focusing in a gas-filled capillary discharge waveguide for high-power laser-plasma applications",* Phys. Plasmas **20**, 093108 (2013). DOI: 10.1063/1.4822333

[5] F.G. Desforges, B.S. Paradkar, M. Hansson, J. Ju, L. Senje, T.L. Audet, A. Persson, S. Dobosz-Dufrénoy, O. Lundh, G. Maynard, P. Monot, J.-L. Vay, C.-G. Wahlström, B. Cros, *"Dynamics of ionization-induced electron injection in the high density regime of laser wakefield acceleration",* Phys. Plasmas **21**, 120703 (2014). DOI: 10.1063/1.4903845

[6] M. Hansson, B. Aurand, X. Davoine, H. Ekerfelt, K. Svensson, A. Persson, C.-G. Wahlström, and O. Lundh, *"Down-ramp injection and independently controlled acceleration of electrons in a tailored laser wakefield accelerator",* Phys. Rev. ST Accel. Beams **18**, 071303 (2015). DOI: 10.1103/PhysRevSTAB.18.071303

[7] C. Thaury, K. Ta Phuoc, S. Corde, P. Brijesh, G. Lambert, S. P. D. Mangles, M. S. Bloom, S. Kneip, and V. Malka, *"Probing electron acceleration and x-ray emission in laser-plasma accelerators",* Phys. Plasmas **20**, 063101 (2013). DOI: 10.1063/1.4810791

[8] J. Vieira, J.L. Martins, V.B. Pathak, R.A. Fonseca, W.B. Mori and L.O. Silva, *"Magnetically assisted self-injection and radiation generation for plasma-based acceleration",* Plasma Phys. Control. Fusion **54**, 124044 (2012). DOI: 10.1088/0741-3335/54/12/124044